2-2

High Enthalpy Flow Workshop

Problem II-1 OREX Configuration

Ichiro NAKAMORI* and Yoshiaki NAKAMURA†

Dept. of Aerospace Engineering, Nagoya University

In this computation, an upwind method with MUSCL type extrapolation was applied to nonequilibrium chemical reacting hypersonic flow around an orbital re-entry experimental (OREX) configuration. The flow solver employed in this computation is based on Steger and Warming's[1] flux-vector splitting (FVS), and classified as a variation of the advection upstream splitting method (AUSM)[4]. It has been confirmed that the present scheme has many good characteristics in the ideal gas flow such as monotonicity for shock wave, robustness for expansion wave, and high resolution for contact discontinuity and shear layer. In order to extend the present scheme to a chemical reacting flow, we used Park's two temperature model for 5 neutral species(N, O, NO, O_2, N_2) with 17 chemical reaction, and the finite volume formulation was employed to discretize the axisymmetric Navier-Stokes equations.

Nomenclature

c	= speed of sound
e	= internal energy per unit volume
E	= total energy per unit volume
e_v	= vibrational energy per unit volume
F	= inviscid flux vector
G	= viscous flux vector
H	= thermochemical source
H	= total enthalpy
p	= pressure
q	= solution vector
u, v, w	= Cartesian velocity components
x, y, z	= Cartesian coordinates
λ	= eigenvalue
ρ	= density
Superscript	
$\pm$	= positive and negative flux contributions
Subscript	
L	= left hand side of the cell interface
R	= right hand side of the cell interface
s	= species

Introduction

We computed a hypersonic flow around OREX configuration under the following assumptions:

free stream velocity: 7450m/s
free stream pressure: 0.169N/m^2
free stream temperature: 186.9K;
the mass fraction of species in free stream:
N_2-79%, O_2-21%.

Moreover, we assumed the flow is laminar and chemically and thermally nonequilibrium. The wall temperature was fixed at 540K. In order to take the thermal nonequilibrium into account, we employed Park's two temperature model, where the translational-rotational modes have the translational temperature, while the vibrational mode has the vibrational temperature. In this study, a 5-species and 17-chemical reaction model is used:

$$O_2 + M \leftrightarrow O + O + M, \quad M = N, NO, O, N_2, O_2$$
$$N_2 + M \leftrightarrow N + N + M, \quad M = N, NO, O, N_2, O_2$$
$$NO + M \leftrightarrow N + O + M, \quad M = N, NO, O, N_2, O_2$$
$$O + NO \leftrightarrow N + O_2,$$
$$O + N_2 \leftrightarrow N + NO.$$

The numerical method is based upon the modified Flux-Vector Splitting to estimate the cell-interface inviscid fluxes, and the Lower-Upper Symmetric Gauss-Siedel (LU-SGS) factorization[6,7] was utilized for the time integration to efficiently solve the system equations in Δ-form.

Governing Equations

A nonequilibrium chemical reacting flow has the system of governing equations with the physical model, which is expressed in the following form:

*Graduate student
†Professor, Aerospace Engineering

$$\frac{\partial \mathbf{q}}{\partial t}+\frac{\partial \mathbf{F}_i}{\partial x_i}=\frac{\partial \mathbf{G}_i}{\partial x_i}+\mathbf{H} \tag{1}$$

where

$$\mathbf{q}=\begin{bmatrix}\rho\\ \rho u\\ \rho v\\ \rho w\\ E\\ \rho_1\\ \vdots\\ \rho_n\\ e_v\end{bmatrix},\ \mathbf{F}_i=\begin{bmatrix}\rho u_i\\ \rho u_1u_i+\delta_{1,i}p\\ \rho u_2u_i+\delta_{2,i}p\\ \rho u_3u_i+\delta_{3,i}p\\ (E+p)u_i\\ \rho_1u_i\\ \vdots\\ \rho_nu_i\\ e_vu_i\end{bmatrix},\ \mathbf{G}_i=\begin{bmatrix}0\\ \tau_{i,1}\\ \tau_{i,2}\\ \tau_{i,3}\\ \tau_{e,i}\\ \rho D_1\frac{\partial \chi_1}{\partial x_i}\\ \vdots\\ \rho D_n\frac{\partial \chi_n}{\partial x_i}\\ \tau_{v,i}\end{bmatrix},\ \mathbf{H}=\begin{bmatrix}0\\ 0\\ 0\\ 0\\ 0\\ H_1\\ \vdots\\ H_n\\ H_v\end{bmatrix}$$

$$E=e+\frac{1}{2}\rho\left(u_1^2+u_2^2+u_2^2\right),$$

and

$$p=p(\rho,e,\rho_1,\ldots,\rho_n,) \tag{2}$$

the solution vector **q** consists of the total density ρ, the momentum components in x, y, and z directions:ρu, ρv, ρw, the total energy E, the species density ρ_s, and the vibrational energy e_v. D_s, X_s, and H_s denote the diffusion coefficients, the mole fraction, and source terms, respectively. These equations include the internal energy e, which can be expressed as the sum of translational-rotational energy e_T and vibrational energy e_v, which are given as

$$e_T=\sum_s \rho_s e_{T_s} \tag{3}$$

$$e_v=\sum_s \rho_s e_{v_s} \tag{4}$$

Numerical Method

Inviscid flux evaluation

The inviscid flux vector in the x direction of the Cartesian coordinates is written as

$$\mathbf{F}=\left[\rho u,\ \rho u^2+p,\ \rho uv,\ \rho uw,\ \rho uH,\ \rho_1 u,\ \cdots,\ \rho_n u,\ e_v u\right]^t \tag{5}$$

where H is the total enthalpy:

$$H=(e+p)/\rho \tag{6}$$

We first describe the cell-interface mass flux formula[8,9], because other fluxes are constructed based upon it. We define the cell-interface mass flux following the FVS formulas for the ideal gas flow, which is given as

$$(\rho u)_{i+1/2}=\left(\rho_L\tilde{\lambda}_1^+ +\rho_R\tilde{\lambda}_1^-\right)+\frac{p_L}{\tilde{c}_L^2}\left(-2\tilde{\lambda}_1^+ +\tilde{\lambda}_2^+ +\tilde{\lambda}_3^+\right)_L +\frac{p_R}{\tilde{c}_R^2}\left(-2\tilde{\lambda}_1^- +\tilde{\lambda}_2^- +\tilde{\lambda}_3^-\right)_R \tag{7}$$

It has been pointed out that FVS schemes[1,2,3] generally produce excessive numerical dissipation for contact discontinuity and shear layer. In order to eliminate such dissipation, we separated pressure contributions from the cell-interface mass flux, because there is no difference of pressure across the contact discontinuity. Then, we introduced the virtual speed of sound instead of the local speed of sound, which is expressed as

$$\begin{aligned}\tilde{c}_L&=c_mK+c_L(1-K)\\ \tilde{c}_R&=c_mK+c_R(1-K)\end{aligned} \tag{8}$$

where

$$c_m=\frac{c_L+c_R}{2} \tag{9}$$

and

$$K=min(p_L,p_R)/max(p_L,p_R) \tag{10}$$

Moreover, the eigenvalues employed in this formula are defined as the polynomials of Mach number, which is redefined by using the virtual speed of sound $\tilde{c}$.

$$\tilde{\lambda}_1^{\pm}=\frac{1}{2}\tilde{c}\left(\tilde{M}\pm\left|\tilde{M}\right|\right) \tag{11a}$$

$$\tilde{\lambda}_2^{\pm}=\begin{cases}\tilde{c}\left[\alpha^{\pm}+\beta^{\pm}\right] & if\ \left|\tilde{M}\right|\le 1\\ \frac{1}{2}\tilde{c}\left(\tilde{M}+1+\left|\tilde{M}+1\right|\right) & othewise\end{cases} \tag{11b}$$

$$\tilde{\lambda}_3^{\pm}=\begin{cases}\tilde{c}\left[\alpha^{\pm}-\beta^{\pm}\right] & if\ \left|\tilde{M}\right|\le 1\\ \frac{1}{2}\tilde{c}\left(\tilde{M}-1+\left|\tilde{M}-1\right|\right) & othewise\end{cases} \tag{11c}$$

where

$$\tilde{M}=\frac{u}{\tilde{c}} \tag{12}$$

and

$$\alpha^{\pm}=\pm\frac{1}{8}\left(\tilde{M}\pm 1\right)^2\left(\tilde{M}^2\mp 2\tilde{M}+3\right) \tag{13}$$

$$\beta^{\pm}=\frac{1}{4}\left(\tilde{M}\pm 1\right)^2\left(2\mp\tilde{M}\right) \tag{14}$$

$\alpha^{\pm}$ and $\beta^{\pm}$ are defined so as to satisfy the restriction of the compatible conditions, which are given as

$$\alpha^+ +\alpha^- =\tilde{M} \tag{15}$$

and

$$\beta^+ +\beta^- =1 \tag{16}$$

These expressions can be extended to nonequilibrium gas flow on the assumption that a speed of sound c is calculated from the eigenvalues included in the Jacobian matrices. As a result, th speed of sound employed in this solver is equivalent to an appropriate frozen speed of sound.

Then, the interface momentum flux can be also expressed by the FVS formula, which is given as

$$\left(\rho u^2+p\right)_{i+1/2}=\tilde{F}_{1,L}^{+}u_L+\tilde{F}_{1,R}^{-}u_R +\frac{1}{2}\left[\left(\tilde{\lambda}_2^+ -\tilde{\lambda}_3^+\right)\frac{p_L}{\tilde{c}_L}+\left(\tilde{\lambda}_2^- -\tilde{\lambda}_3^-\right)\frac{p_R}{\tilde{c}_R}\right] \tag{17}$$

where

$$\tilde{F}_1^{\pm} = \rho\,\tilde{\lambda}_1^{+} + \frac{p}{\tilde{c}^2}\left(-2\tilde{\lambda}_1^{\pm} + \tilde{\lambda}_2^{\pm} + \tilde{\lambda}_3^{\pm}\right) \tag{18}$$

To prevent the scheme from having some difficulties at the stagnation point, $\tilde{\lambda}_1$ would be redefined as

$$\tilde{\lambda}_1^{\pm} = \begin{cases} \frac{1}{2}\tilde{c}\left(\tilde{M} \pm \left|\tilde{M}\right|\right) & \text{if } \left|\tilde{M}\right| \geq \varepsilon \\ \frac{1}{2\varepsilon}\tilde{c}\left(\tilde{M} \pm \varepsilon\right)^2 & \text{otherwise} \end{cases} \tag{19}$$

where

$$\varepsilon = 0.2\frac{min(p_L, p_R)}{max(p_L, p_R)} \tag{20}$$

ε is a small empirical value depending on the pressure gradient. However, this modification results in dissipative solution for the stationary contact discontinuity. Then, for the practical use, density was calculated with the upstream values as follows:

$$\begin{aligned} &\tilde{\rho}_L = \rho_L,\ \tilde{\rho}_R = \rho_L && \text{if } \left|\tilde{M}\right| \leq \varepsilon \text{ and } u_{i+1/2} \geq 0 \\ &\tilde{\rho}_L = \rho_R,\ \tilde{\rho}_R = \rho_R && \text{if } \left|\tilde{M}\right| \leq \varepsilon \text{ and } u_{i+1/2} < 0 \\ &\tilde{\rho}_L = \rho_L,\ \tilde{\rho}_R = \rho_R && \text{otherwise} \end{aligned} \tag{21}$$

Then, we utilized the advection upstream splitting method(AUSM)[4,5] for tangential momentum fluxes, energy flux, species mass flux, and vibrational energy flux, which are expressed according to the sign of the cell-interface mass flux previously obtained. The fluxes are written as

$$(\rho uv)_{i+1/2} = \frac{1}{2}(\rho u)_{i+1/2}(v_L + v_R) - \frac{1}{2}\left|(\rho u)_{i+1/2}\right|(v_R - v_L) \tag{22}$$

$$(\rho uw)_{i+1/2} = \frac{1}{2}(\rho u)_{i+1/2}(w_L + w_R) - \frac{1}{2}\left|(\rho u)_{i+1/2}\right|(w_R - w_L) \tag{23}$$

$$(\rho uv)_{i+1/2} = \frac{1}{2}(\rho u)_{i+1/2}(H_L + H_R) - \frac{1}{2}\left|(\rho u)_{i+1/2}\right|(H_R - H_L) \tag{24}$$

$$(\rho uv)_{i+1/2} = \frac{1}{2}(\rho u)_{i+1/2}(e_{v_L} + e_{v_R}) - \frac{1}{2}\left|(\rho u)_{i+1/2}\right|(e_{v_R} - e_{v_L}) \tag{22}$$

A piecewise linear interpolation was used with a minimum-modulus (minmod) TVD limiter in such a way that these inviscid fluxes have the second-order accuracy in space.

Transport Coefficients

In order to evaluate the transport coefficients, we use Yos's formulas based upon Chapman-Enskog's first approximation. To simplify the estimation of the collision integral in Yos's formulas, we invoke Chapman-Cowling's formulas for viscosity and diffusion coefficients with Wilke's empirical formulas. Comparing these formulas with Yos's one, a compact expression is available for the collision integral, leading to the easily computed expression for the transport coefficients.

Translational Vibrational Energy Relaxation

In this study, the relaxation model introduced by Landau and Teller for the vibrational-electronic excitation energy was employed, where the relaxation time can be calculated in Millikan-White's[14] empirical correlation with Park's[10] correction at high temperature.

Numerical Results

To verify the calculation method mentioned above, we computed the flow field around OREX configuration, whose diameter is 6.8m. Figure 1 shows the grid system of 32×64, where the minimum value of $\Delta\eta$ is 1×10^{-4} near the wall. The OREX configuration has the following flight conditions :

free stream velocity: 7450m/s;
free stream temperature: 186.9K;
free stream pressure: 0.169N/m^2;
mass fraction of species in free stream:
N_2-79%, O_2-21%.

These data were employed at the High Enthalpy Flow Workshop. In addition, the body surface temperature was fixed at 540K along with the assumption of a non-catalytic wall. Steady solutions were calculated with the residual reduced by three order of magnitude from the initial one. Figures 2-6 show pressure, translational-rotational temperature, and vibrational temperature contours along with the mole fraction of species, translational-rotational temperature and vibrational temperature profiles along the stagnation stream line. The present scheme can capture a strong shock wave with no oscillation in the fields of pressure, translational-rotational temperature, vibrational temperature, and mole fraction of species. It should be noted that the present scheme does not need the special procedure to protect the numerical oscillation of the bow shock wave near the stagnation stream line, called the carbuncle phenomenon[4].

Figures 7 and 8 show pressure and heat flux distributions along the body surface. The heat flux at the stagnation was 41.6kW/m^2. These value must be verified by comparing with the experimental data, because it is difficult to estimate the heat flux distribution on the body surface.

Conclusion

In the present study, an improved Flux-Vector Splitting method was applied to a nonequilibrium chemical reacting hypersonic flow around OREX configuration selected at the High Enthalpy Flow Workshop. The results show the validity of the numerical method in shock capturing, monotonicity, and robustness. Further comparison between numerical solution and experimental data is required.

Acknowledgment

We would like to acknowledge to Dr. I. S. Men'shov for his help to compute a chemical reacting flow.

References

(1) Steger, J. L. and Warming, R. F., "Flux Vector Splitting of the Inviscid Gasdynamic Equations with Application to Finite Difference Methods," *J. Comput. Phys.*, Vol. 40, 1981, pp. 263-293.

(2) Van Leer, B., "Flux–Vector Splittings for the Euler Equations," Lecture Notes in Physics, Vol. 170, 1982, pp. 507–512.

(3) Hänel, D. and Schwance, "An Implicit Flux–Vector Splitting Scheme for the Computation of Viscous Hypersonic Flow," AIAA Paper 89–0274, 1989.

(4) Liou, M. S. and Steffen, C. J., "A New Flux Splitting Scheme," *J. Comput. Phys.* Vol. 107, 1993, pp. 23-39.

(5) Wada, Y. and Liou, M. S., "A Flux Splitting Scheme With High–Resolution and Robustness for Dis-continuities," NASA TM 106452, 1994.

(6) Jameson, A. and Yoon, S., "Lower-Upper Implicit Schemes with Multiple Grids for the Euler Equations," *AIAA Journal*, Vol. 25, 1987, pp. 929-935.

(7) Jameson, A. and Turkel, E., "Implicit Schemes and LU Decompositions," *Math. of Comput.* 37, pp. 385-397, 1981.

(8) Nakamori, I. and Nakamura, Y., "An Upwind Scheme Based on the Flux-Vector Splitting," AIAA Paper 95-0471, 1995.

(9) Nakamori, I. and Nakamura, Y., "An Upwind Scheme for the Inviscid and Viscous Hypersonic Flow," AIAA Paper 95-1732, 1995.

(10) Park, C., "Assessment of Two-Temperature Kinetic Model for Ionizing Air," AIAA Paper 87-1574, 1987

(11) Gnoffo, P. A., Gupta, R. N., and Shinn, J. L., "Conservation Equations and Physical Models for Hypersonic Air Flows in Thermal and Chemical Nonequilibrium," NASA TP 2867, 1989.

(12) Hornung, H. G. and Wen C.-Y.,"Nonequilibrium Dissociating Flow over Spheres," AIAA Paper 95-0091, 1995.

(13) Rock, S. G. and Tramel, R. W., "A Three-Dimensional Thermo-Chemical Nonequilibrium Chimera Flow Solver for Moving Grids, Part I:Steady State," AIAA Paper 95-0151, 1995.

(14) Millikan, R. C. and White, D. R.,"Systematics of Vibrational Relaxation," *J. Chem. Phys.*, 39, pp. 3209-3213, 1963.

(15) White, F. M., "Viscous Fluid Flow," McGraw-Hill Book Company, pp. 27-36, 1974.

(16) Vincenti, W. G. and Kruger, C. H.,"Introduction to Physical Gas Dynamics," Krieger Pub. Company, pp. 197-245, 1993.

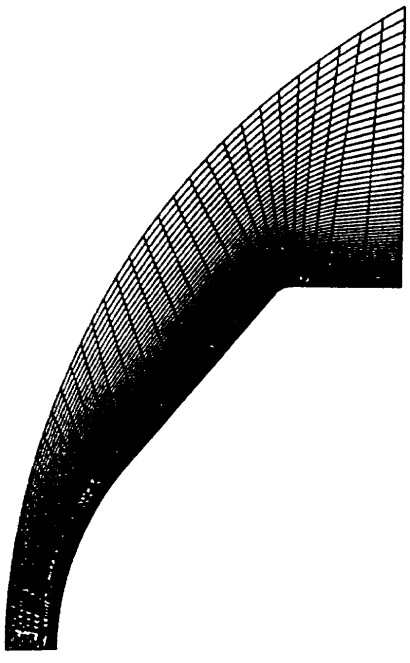

Figure 1 Grid configuration: 32×64

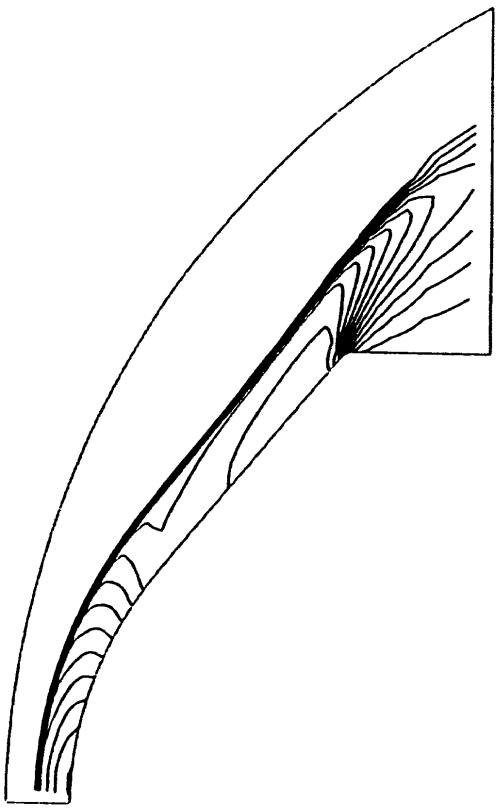

Figure 2 Pressure contours.

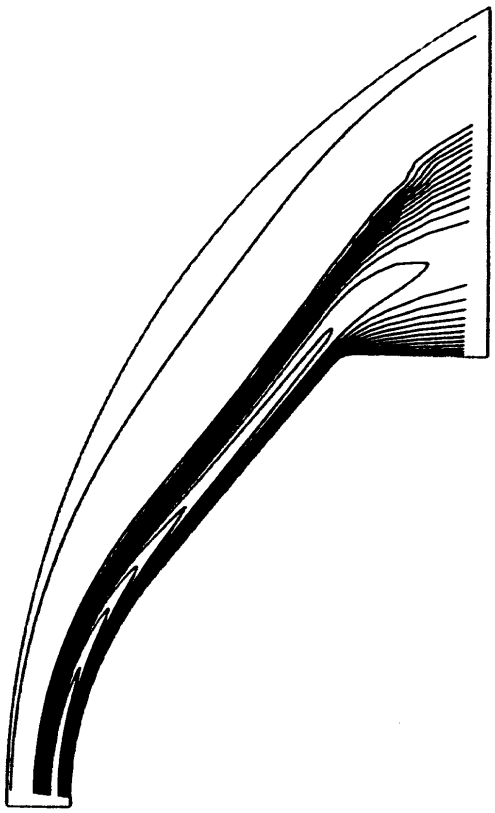

Figure 4 Vibrational temperature contours.

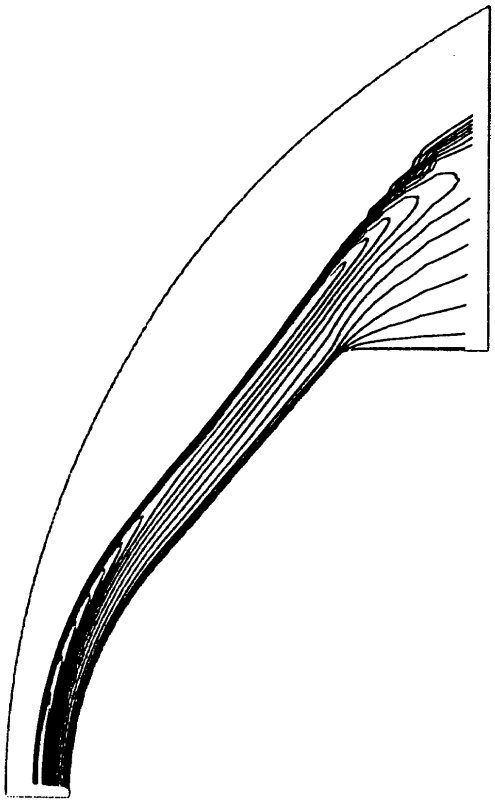

Figure 3 Translational temperature contours.

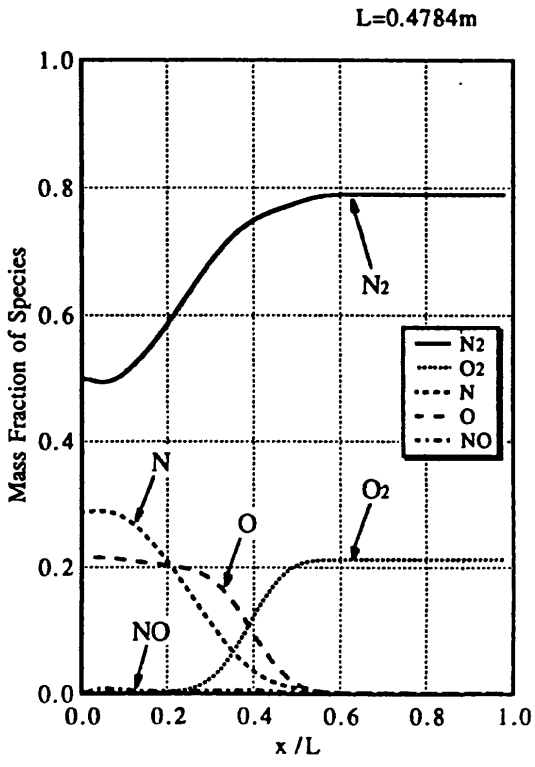

Figure 5 Mass fraction of species distributions along the stagnation stream line.

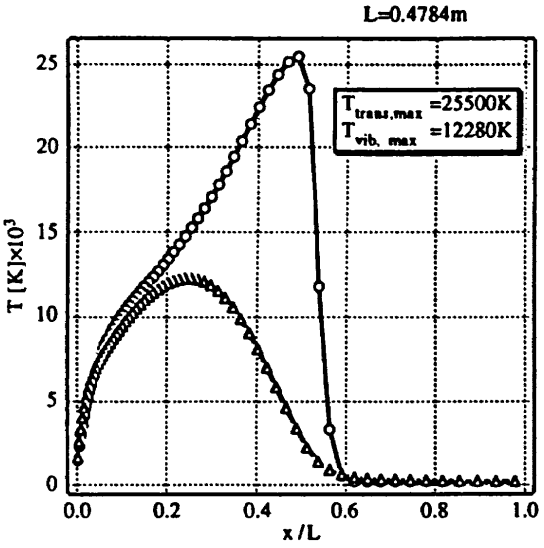

Figure 6 Translational and vibrational temperature distributions along the stagnation stream line.

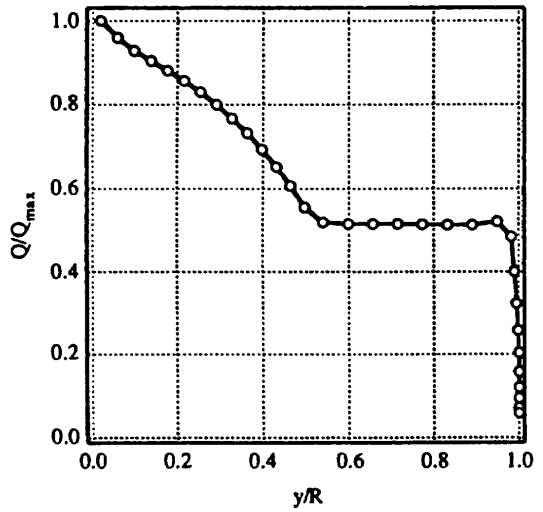

Figure 7 Heat flux distributions along the body surface.

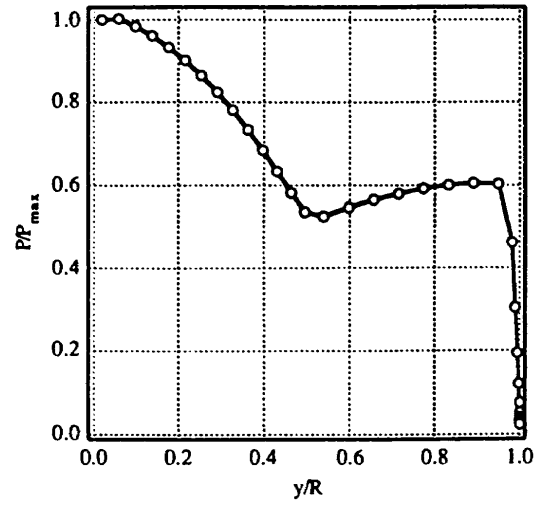

Figure 8 Pressure distributions along the body surface.